2021 29th Mediterranean Conference on Control and Automation (MED)
June 22-25, 2021. Bari, Puglia, Italy

2021 29th Mediterranean Conference on Control and Automation (MED) | 978-1-6654-2258-1/20/$31.00 ©2021 IEEE | DOI: 10.1109/MED51440.2021.9480270

Predictive Control for Zonal Congestion Management of a Transmission Network

Duc-Trung Hoang, Sorin Olaru, Alessio Iovine, Jean Maeght, Patrick Panciatici, Manuel Ruiz

***Abstract*— Nowadays power transmission networks need to face congestion problems casted on the form of control problems in the presence of uncertainty. Transmission system operators (TSOs) as the French one (RTE) want to avoid power overloads on the lines by focusing on optimal management of battery systems and, if necessary, renewable production curtailments. Target of the present paper is to use a model-based optimal control approach for managing the power flow in a sub-area of a transmission network by the utilisation of storage devices and partial curtailment of the renewable power. Model Predictive Control (MPC) framework is used to include power constraints validation from the design stage. A series of hypothesis are analysed and the principles of congestions management functioning are illustrated through simulations.**

Keywords: Power transmission network, MPC, energy storage, partial power curtailment.

I. Introduction

Nowadays, the utilisation of renewable power is increasing fast due to its competitive cost, positive environmental impact, and incredible efficiency. However, its introduction complicates power systems operation and management, as it affects stability, as small fluctuations in distributed generation may impact power systems' performance. Consequently, Transmission System Operators (TSOs) as the French RTE deal with a growing number of difficulties related to power congestion on transmission lines [1]. One of the possible solutions under consideration is to use optimization-based approaches to manage sub-transmission areas (zones) by the use of storage devices and renewable power curtailments if needed. In order to build a resilient and decentralized system composed by zones, only a local description of each zone is considered for control purposes: the connection with the remaining network is defined as a perturbation acting on the zone. In [2], the authors provide a dynamical model based on Power Transfer Distribution Factor (PTDF) (see [3], [4]) that extends previous modeling for zones that only allowed on/off decision on power curtailment [5], [6]. The proposed model targets the possible use of model-based optimal control to manage the subtransmission area congestion situation.

The main challenge in controlling an isolated zone is to operate local control actions with respect to the global power flow taking place at the boundaries of the zone. This local information translates at the mathematical model in terms of uncertainty, and subsequently affects the decision making. The goal of the present paper is to validate the utilisation of a real-time control strategy as Model Predictive Control (MPC) [7] to operate the storage devices and partially curtail power from renewables whenever the constraints on the operation of power lines are violated [8], [9]. A simplified not-delayed version of the model in [2] is used to describe the dynamical system model proposed for model-based control, and the simulation tool MATPOWER [10] with the full French grid data [11] is set to simulate the power transmission line under various scenarios, using real data for renewable power generation. While the main contribution is the mathematical description of the design framework, an industrial case study on the control of a zone will be considered for the illustration of the main congestion management features. Figure 1 represents a geographical region close to Dijon, France. It is composed by six nodes with loads, generators and a battery. Target of the MPC tuning is to appropriately model and control the generated power on the nodes and their influence on the branches of the electrical transmission model. The following notations will be used along the developments:

- $\mathcal{Z}^N$ is the set of nodes in the considered zone; n^N is its cardinality. P_n^T is the power generated in the transmission network flowing from the external network to the node $n \in \mathcal{Z}^N$ of the zone of interest.
- $\mathcal{Z}^C \subset \mathcal{Z}^N$ is the set of nodes where the curtailment of the generated power is allowed; n^C is its cardinality. P_n^G is the generated power, while P_n^C is the curtailed one at node $n \in \mathcal{Z}^C$. P_n^A is the available renewable power that can be generated each sampling time.
- $\mathcal{Z}^B \subset \mathcal{Z}^N$ is the set of nodes with a battery; n^B is its cardinality. P_n^B is the power injected from the battery on node $n \in \mathcal{Z}^C$, while E_n^B describes the battery energy at the same node.
- $\mathcal{Z}^L \subset \{(i,j) \in \{1,...,n^N\} \times \{1,...,n^N\}\}$ is the set of power lines in the zone; n^L is its cardinality. F_{ij} represents the power flow on the line ij.

The paper is organized as follows. Section II introduces the considered control-oriented modeling and Section III describes the MPC setting. Simulations validating the control approach are carried out in Section IV, while concluding

Duc-Trung Hoang, Sorin Olaru and Alessio Iovine are with the Laboratory of Signals and Systems (L2S), *CentraleSupélec, Paris-Saclay University*, Gif-sur-Yvette, France. Email: {trung.hoang-duc, sorin.olaru, alessio.iovine}@centralesupelec.fr

Jean Maeght, Patrick Panciatici, Manuel Ruiz are with French Transmission System Operator, *Réseau de Transport d'Électricité* (RTE), Paris, France. Email: {name.surename}@rte-france.com

This work was carried out within the CPS4EU project, which has received funding from the ECSEL Joint Undertaking (JU) under grant agreement No 826276. The JU receives support from the European Union's Horizon 2020 research and innovation programme and France, Spain, Hungary, Italy, Germany. The proposed results reflect only the authors' view. The JU is not responsible for any use that may be made of the information the present work contains.

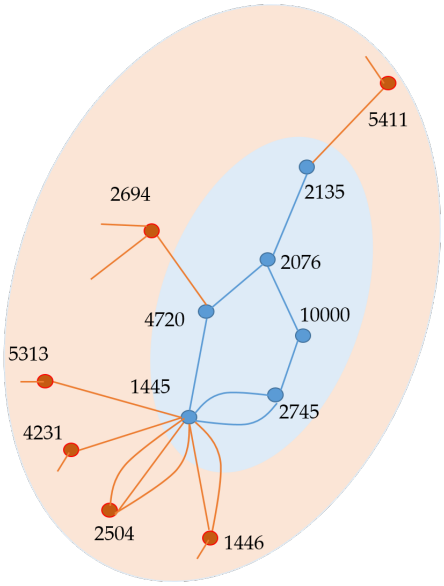

Fig. 1. The considered zone (blue nodes) and its connection to the entire power network (red nodes). The power flow interaction among the blue nodes and the red nodes is described as an uncontrolled generated/absorbed power and thus assimilated as disturbances in the decision making process.

remarks are outlined in Section V.

Notation: The operator *diag* describes a diagonal matrix composed by the considered elements. The operator *col* assigns a single column vector by the aggregation of matrix columns, i.e.. given m vectors $s_i \in \mathbb{R}^n$, $i = 1, ..., m$, the resulting vector $s = col[s_i], i = 1, 2, \ldots, m$, will be:

$$s = col[s_i] = [\ s_1^T\ \ s_2^T\ \ ...\ \ s_m^T\ ]^T \in \mathbb{R}^{nm}. \tag{1}$$

II. Modeling

We revisit the linear model based on Direct Current (DC) approximation described in [2] and, for facilitating the presentation, present the delay-free case. In view of transmission network modeling, the following working hypothesis are considered:

1) each generator produces the maximum available renewable power or the maximum allowed one;
2) only a higher level controller can decrease the power curtailment set-points. For this reason, the proposed controller deals only with curtailment increase;
3) the State of Charge (SOC) of the battery is updated each second by a SCADA system. Together with the considered high voltage, these short time intervals with respect to longer ones taken here into account for control purposes, both sampling and prediction horizon, allow to neglect losses due to the battery system (conversion, cooling and transformers). A different control level is supposed to manage the SOC with respect to longer time horizons [12];
4) the loads are constant.

The state variables of the energy transmission are: the power flows on the lines F_{ij}, the generated power P_n^G, the curtailed power P_n^C and the battery power output P_n^B, respectively, and the energy of the batteries E_n^B. The control inputs are the power variations ΔP_n^B and ΔP_n^C. Finally, the power variation ΔP_n^G of the generated power P_n^G is a filtered disturbance acting on the system. It is known at instant k based on the state, control input and context information within the zone (available power). Indeed, the actually available power P_n^A is not part of the state vector. We suppose it is communicated to the TSO at each sampling time, together with the power variation ΔP_n^A. Consequently, the value of ΔP_n^G is implicitly defined with respect to the communicated values of P_n^A, ΔP_n^A, and the stored value of P_n^G with respect to P_n^C. The disturbance ΔP_n^T is unknown as it involves the information outside the operated zone.

The dynamical model is:

$$\begin{cases} F_{ij}(k+1) = & F_{ij}(k) + \sum_{n\in\mathcal{Z}^B} b_{ij}^n \Delta P_n^B(k) \\ & + \sum_{n\in\mathcal{Z}^C} b_{ij}^n \left[\Delta P_n^G(k) - \Delta P_n^C(k)\right] \\ & + \sum_{n\in\mathcal{Z}^N} b_{ij}^n \Delta P_n^T(k),\ \forall\ (ij) \in \mathcal{Z}^L \\ P_n^C(k+1) = & P_n^C(k) + \Delta P_n^C(k),\ \forall\ n \in \mathcal{Z}^C \\ P_n^B(k+1) = & P_n^B(k) + \Delta P_n^B(k),\ \forall\ n \in \mathcal{Z}^B \\ E_n^B(k+1) = & E_n^B(k) - Tc_n^B[P_n^B(k) + \Delta P_n^B(k)], \\ & \forall\ n \in \mathcal{Z}^B \\ P_n^G(k+1) = & P_n^G(k) + \Delta P_n^G(k) - \Delta P_n^C(k), \\ & \forall\ n \in \mathcal{Z}^C \end{cases} \tag{2}$$

where b_{ij}^n are constant parameters given by PTDF computation, and c_n^B are constant power reduction factors for the batteries. In particular, the term $\Delta P_n^G(k)$, is defined as

$$\Delta P_n^G(k) = \min\left(f_n^G(k), g_n^G(k)\right), \tag{3}$$

$$f_n^G(k) = P_n^A(k) + \Delta P_n^A(k) - P_n^G(k) + \Delta \hat{P}_n^C(k), \tag{4}$$

$$g_n^G(k) = \overline{P}_n^G - P_n^C(k) - P_n^G(k). \tag{5}$$

where $\overline{P}_n^G > 0$ is the maximum installed capacity of the power that can be generated by the n renewable power plant, with $n \in \mathcal{Z}^C$, and the value of $\Delta \hat{P}_n^C(k)$ is defined in the following. According to this, the proposed modeling allows for the possibility to pre-compute the term $\Delta P_n^G(k)$, based on values of $P_n^A(k)$, $P_n^G(k)$, $P_n^C(k)$, $\Delta P_n^A(k)$ and $\Delta P_n^C(k)$, while maintaining the system linear via the offline computation of the $\min(.)$ and consequently reducing the computational effort of dedicated model-based predictive control laws. The main drawback is related to the term $\Delta \hat{P}_n^C(k)$. Whenever this is an independent variable at the pre-computation time of sampling instant k, i.e. whenever $\Delta \hat{P}_n^C(k) = \Delta P_n^C(k)$, then model (2) is implicitly nonlinear.

To avoid this implicit dependence in (2), a prediction-correction mechanism can be used, in particular for control design. Indeed, one can purposely consider a predicted value, e.g. $\Delta \hat{P}_n^C(k) = 0$, in (4) and dissociate it from the actual selection of $\Delta P_n^C(k)$, which is the control input to be fixed at time k. The linearity of the prediction model is preserved and its evolution can be corrected once $\Delta P_n^C(k)$ is chosen. This mechanism implies a model mismatch in between the prediction and the correction phase, whenever $\Delta P_n^C(k) \neq \Delta \hat{P}_n^C(k)$.

To describe the model in a compact form, we define:

$$F = col[F_{ij}],\ \forall\ (i,j) \in \mathcal{Z}^L; \tag{6a}$$
$$P^C = col[P_n^C],\ \Delta P^C = col[\Delta P_n^C],\ \forall\ n \in \mathcal{Z}^C; \tag{6b}$$
$$P^B = col[P_n^B],\ \forall\ n \in \mathcal{Z}^B; \tag{6c}$$
$$E^B = col[E_n^B],\ \Delta P^B = col[\Delta P_n^B],\ \forall\ n \in \mathcal{Z}^B; \tag{6d}$$
$$\Delta P^T = col[\Delta P_n^T],\ \forall\ n \in \mathcal{Z}^N; \tag{6e}$$
$$P^G = col[P_n^G],\ \Delta P^G = col[\Delta P_n^G],\ \forall\ n \in \mathcal{Z}^C. \tag{6f}$$

According to (6a)-(6f), the resulting linear system is described as

$$\begin{aligned} x(k+1) =& Ax(k) + B_C u_C(k) + B_B u_B(k) \\ &+ D_w w(k) + D_\zeta \zeta(k) \end{aligned} \tag{7}$$

where

$$x(k) = [F(k)\ \ P^C(k)\ \ P^B(k)\ \ E^B(k)\ P^G(k)]^T, \tag{8}$$
$$u_C(k) = \Delta P^C(k),\ \ u_B(k) = \Delta P^B(k), \tag{9}$$
$$w(k) = \Delta P^G(k),\ \ \zeta(k) = \Delta P^T(k), \tag{10}$$

$$A = \begin{pmatrix} \mathbb{1}_{\mathbf{n^L}\times\mathbf{n^L}} & \mathbb{0}_{\mathbf{n^L}\times\mathbf{n^C}} & \mathbb{0}_{\mathbf{n^L}\times\mathbf{n^B}} & \mathbb{0}_{\mathbf{n^L}\times\mathbf{n^B}} & \mathbb{0}_{\mathbf{n^L}\times\mathbf{n^C}} \\ \mathbb{0}_{\mathbf{n^C}\times\mathbf{n^L}} & \mathbb{1}_{\mathbf{n^C}\times\mathbf{n^C}} & \mathbb{0}_{\mathbf{n^C}\times\mathbf{n^B}} & \mathbb{0}_{\mathbf{n^C}\times\mathbf{n^B}} & \mathbb{0}_{\mathbf{n^C}\times\mathbf{n^C}} \\ \mathbb{0}_{\mathbf{n^B}\times\mathbf{n^L}} & \mathbb{0}_{\mathbf{n^B}\times\mathbf{n^C}} & \mathbb{1}_{\mathbf{n^B}\times\mathbf{n^B}} & \mathbb{0}_{\mathbf{n^B}\times\mathbf{n^B}} & \mathbb{0}_{\mathbf{n^B}\times\mathbf{n^C}} \\ \mathbb{0}_{\mathbf{n^B}\times\mathbf{n^L}} & \mathbb{0}_{\mathbf{n^B}\times\mathbf{n^C}} & -A_b & \mathbb{1}_{\mathbf{n^B}\times\mathbf{n^B}} & \mathbb{0}_{\mathbf{n^B}\times\mathbf{n^C}} \\ \mathbb{0}_{\mathbf{n^C}\times\mathbf{n^L}} & \mathbb{0}_{\mathbf{n^C}\times\mathbf{n^C}} & \mathbb{0}_{\mathbf{n^C}\times\mathbf{n^B}} & \mathbb{0}_{\mathbf{n^C}\times\mathbf{n^B}} & \mathbb{1}_{\mathbf{n^C}\times\mathbf{n^C}} \end{pmatrix}$$

$$B_C = \begin{pmatrix} -M_c & \mathbb{1}_{\mathbf{n^C}\times\mathbf{n^C}} & \mathbb{0}_{\mathbf{n^B}\times\mathbf{n^C}} & \mathbb{0}_{\mathbf{n^B}\times\mathbf{n^C}} & -\mathbb{1}_{\mathbf{n^C}\times\mathbf{n^C}} \end{pmatrix}^T$$

$$B_B = \begin{pmatrix} M_b & \mathbb{0}_{\mathbf{n^C}\times\mathbf{n^B}} & \mathbb{1}_{\mathbf{n^B}\times\mathbf{n^B}} & -A_b & \mathbb{0}_{\mathbf{n^C}\times\mathbf{n^B}} \end{pmatrix}^T$$

$$D_w = \begin{pmatrix} M_c & \mathbb{0}_{\mathbf{n^C}\times\mathbf{n^C}} & \mathbb{0}_{\mathbf{n^B}\times\mathbf{n^C}} & \mathbb{0}_{\mathbf{n^B}\times\mathbf{n^C}} & \mathbb{1}_{\mathbf{n^C}\times\mathbf{n^C}} \end{pmatrix}^T$$

$$D_\zeta = \begin{pmatrix} M_t & \mathbb{0}_{\mathbf{n^C}\times\mathbf{n^N}} & \mathbb{0}_{\mathbf{n^B}\times\mathbf{n^N}} & \mathbb{0}_{\mathbf{n^B}\times\mathbf{n^N}} & \mathbb{0}_{\mathbf{n^C}\times\mathbf{n^N}} \end{pmatrix}^T$$

with $A_b = diag[Tc_n^B],\ \forall\ n \in \mathcal{Z}^B$, and M_c, M_b and M_t that are composed by the elements b_{ij}^n obtained by the PTDF computation described in (2). The k^{th} line in these matrices corresponds to the PTDF of the k^{th} line of F_{ij} at nodes where generation can be curtailed, at nodes where a battery is installed or at nodes where the injections may vary, respectively.

We remark that reactive voltage aspects are not considered in this work. This modeling is adapted to identify in real-time the need for acting on curtailment or storage charge/discharge. Alternate Current (AC) feasibility is a consequence of online updates of $cos(\phi)$ from active power and current real-time measurements, where $cos(\phi)$ is the usual power/current ratio at each bus.

III. Closed-loop optimization-based control

The congestion management builds the operational strategy by acting on the available levers (control inputs):

- storage in the batteries $u_B(k)$;
- power curtailment $u_C(k)$;
- topological modifications - modelled by time-varying transition matrix A in (7) (not considered here).

The mathematical model described in Section II is instrumental in the choice of the control inputs based on a optimization criterion. At the same time, the operational constraints related to the congestion need to be considered in the optimization problem from the design stage. Adding to this picture the restricted information available with respect to the produced/consumed power ahead of time $(w(k+i), i > 0)$ or at the interconnection with the considered zone $(\zeta(k+i))$, we obtain the complete design framework.

A. Feedback control strategy description

The congestion management has to answer in real-time to the potential violation of the physical constraints by corrective actions on the level of the storage and the production limitations. The fundamental relationship (balance) between the power generation and consumption induces variations on the power flows transitioning the power network. These dynamical evaluations are subject to uncertainties and they need to be monitored (measurements, estimations, predictions) in order to extract the information needed for the control synthesis.

The essential information available or commutable based on direct processing at each sampling instant k is:

- The power flows on the lines $F_{ij}(k)$ can be measured or estimated;
- The power curtailment $P_n^C(k)$ is known, as it based on past congestion management decisions and the maximal production in each node of the considered zone.
- The battery power $P_n^B(k)$ is measured, and is operated based on the battery storage control signals. It can be translated in terms of the energy stored in the battery;
- The generated/consumed power in each of the nodes is the sensitive quantity in terms of information handling. As discussed in the previous section, it builds on power available (measured in the past but not available at time instant k), the maximal power on the nodes and decisions on power curtailment.

This discussion on the available information triggers a more elaborated discussion on the uncertainty and its propagation along the predictions. At the current time instant k, the uncertainty is concentrated on the evolution of the generated power P_n^G for each node and can be resumed by the interdependence:

$$\Delta P_n^G(k) = \Delta P_n^G(\Delta P_n^A(k), \Delta P_n^C(k)). \tag{11}$$

Clearly, the decision on the power curtailment is subject to uncertainty as long as it is not possible to exploit the aposteriori information. Thus $\Delta P_n^G(k)$ is unknown in:

$$\Delta P_n^C(k) = \Delta P_n^C(\Delta P_n^G(k)).$$

In these conditions one needs to rely on the predictions:

$$\Delta P_n^C(k) = \Delta P_n^C(\Delta \hat{P}_n^G(k))$$

which can be further developed as:

$$\Delta P_n^C(k) = \Delta P_n^C(\Delta \hat{P}_n^A(k), \Delta \hat{P}_n^C(k)). \tag{12}$$

where $\Delta \hat{P}_n^A(k)$ and $\Delta \hat{P}_n^C(k)$ are the predicted/estimated values for $\Delta P_n^A(k)$ and $\Delta P_n^C(k)$, respectively. At the time

instant k, if the information on $\Delta P_n^A(k)$ is not available close to real-time, this uncertainty can be handled based on extrapolations[1]. With respect to $\Delta \hat{P}_n^C(k)$, its impact can be handled based on a prediction-correction mechanism. More important, if the uncertainty is already present at time instant k, its impact will be reiterated along the predictions as long as the same ingredients will have to be manipulated without prior information on ΔP_n^A and $\Delta \hat{P}_n^C$. Despite the jeopardizing effect of the uncertainty on the prediction, it has to be noticed that the control lever offered by the power curtailment is able to mitigate the uncertainty impact if the physical constraints are under threat as long as there always exist a curtailment able to retrieve a level of power generation satisfying the constraints.

B. Mathematical formation of the real-time optimization

Let us define the (constant) upper and lower bounds of each variable using the following notation: $L_{ij} > 0$, $\overline{P}_n^G > 0$, $\overline{P}_n^B > 0$, $\underline{P}_n^B < 0$, $\overline{E}_n^B > 0$, $\underline{E}_n^B > 0$. Then,

$$\overline{L} = col[L_{ij}], \forall\ (i,j) \in \mathcal{Z}^L; \tag{13a}$$

$$\underline{P}^B = col[\underline{P}_n^B],\ \overline{P}^B = col[\overline{P}_n^B],\ \forall\ n \in \mathcal{Z}^B; \tag{13b}$$

$$\underline{E}^B = col[\underline{E}_n^B],\ \overline{E}^B = col[\overline{E}_n^B],\ \forall\ n \in \mathcal{Z}^B; \tag{13c}$$

$$\overline{P}^G = col[\overline{P}_n^G],\ \forall\ n \in \mathcal{Z}^C. \tag{13d}$$

Consequently, supposing the disturbances to be bounded, the constraints are:

$$-\overline{L} \leq F(k) \leq \overline{L},\quad \mathbb{0}_{\mathbf{n^C \times 1}} \leq P^C(k) \leq \overline{P}^G, \tag{14a}$$

$$\underline{P}^B \leq P^B(k) \leq \overline{P}^B,\quad \underline{E}^B \leq E^B(k) \leq \overline{E}^B, \tag{14b}$$

$$\mathbb{0}_{\mathbf{n^C \times 1}} \leq P^G(k) \leq \overline{P}^G,\quad \mathbb{0}_{\mathbf{n^C \times 1}} \leq \Delta P^C(k) \leq \overline{P}^G, \tag{14c}$$

$$\underline{P}^B - \overline{P}^B \leq \Delta P^B(k) \leq \overline{P}^B - \underline{P}^B. \tag{14d}$$

The cost function aims to select a *unique* solution within the feasible domain. At each prediction step it involves the weighted sum of quadratic terms involving:

- setpoint tracking: seldom used (thus having the lowest weighting), mainly to maintain the battery storage in the neighborhood of a *safety* pre-defined level.
- penalty on the control action related to the power curtailment.
- penalty on the control action related to the battery storage.

Let us consider the semidefinite positive matrices Q, R_G and R_B to be the weight matrices with respect to x, u_C and u_B, respectively. Over a N step prediction window, the cost function is defined as:

$$J(k) = \sum_{i=1}^{N} ||x(k+i) - x_r||_Q^2 + \sum_{i=0}^{N-1} ||u_C(k+i)||_{R_G}^2 + \sum_{i=0}^{N-1} ||u_B(k+i)||_{R_B}^2 \tag{15}$$

[1]The simplest alternatives for estimation would be to use a value $\Delta \hat{P}_n^A(k)$, where $\Delta \hat{P}_n^A(k) = \Delta P_n^A(k-1)$ or $\Delta \hat{P}_n^A(k) = 0$

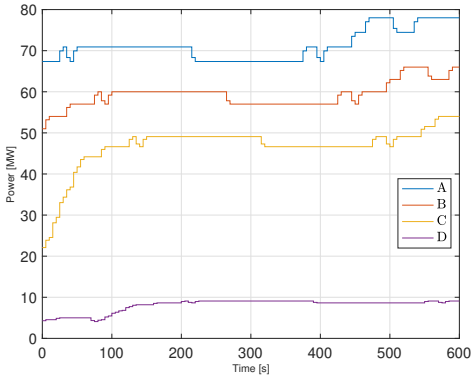

Fig. 2. The available power for generators. A) node 1000; B) node 2076; C) node 2745; D) node 4720.

Based on the cost function, the constraints related to the dynamics and the physical constraints, the receding-horizon optimization is:

$$\mathcal{O}(k) = \arg \min_{u_G(k), u_B(k), \ldots, u_G(k+N-1), u_B(k+N-1)} J(k)$$
$$s.t.\ (7), (14)\ for\ \ k, k+1, \ldots k+N \tag{16}$$

Before analysing the potential of the methodology by means of numerical results, few design details can be underlined. The control strategy targets the use of the power flexibility provided by the storage device acting as a buffer, and to (partially) curtail power generation only if needed. This aspect can be tuned by adjusting the weightings R_B and R_G in (15). From the structure point of view, *the prediction model is linear*, but this comes at the price of a model mismatch in the evaluation (estimation) of the power increments in (3) before the resolution of (16). An alternative with an improved fidelity of prediction but a slightly more complex prediction model involving integer variables has been discussed in [2]. Finally, given the uncertainty of the estimation for the power generation, the use of long prediction horizons without anticipatory information is detrimental and can lead to cautious control, which is deleterious for the global use of the transmission network.

IV. Simulations

The considered zone include six nodes, seven branches, four generators among nodes, and one battery. Then $n^L = 7$, $n^C = 4$ and $n^B = 1$. Maximum power flow on each branch is 45MW (seasonal thermal rating). The considered four power generators have maximum installed power of 78 MW, 66 MW, 54 MW, and 10 MW respectively, while the battery is a 10 MW one. We consider the battery power output not to impact on the stored energy. Figure 2 depicts the scenario of available power at the generators side over the considered simulation time. The power flow solution available in MATPOWER (*runpf*) is used to simulate the AC power flow on the more than 6000 buses of the whole French network [2], while the control algorithms are implemented in MATLAB and YALMIP [13]. The function *runpf* does not simulate a dynamical system, and its utilisation generates a succession of steady states. For the considered application, it is possible to compare them to a time domain simulation.

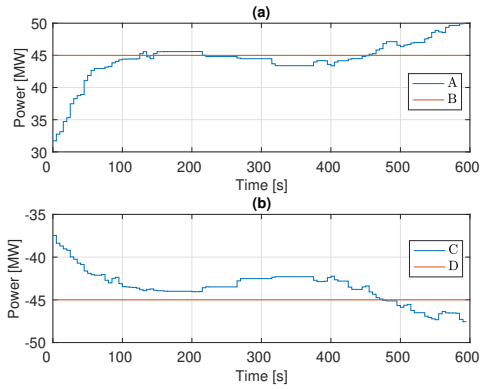

Fig. 3. The power flow on the branches in the open-loop simulation: A) between buses 2745 and 1445; C) between buses 2135 and 2076; B) The maximum power value 45; D) The minimum power value -45.

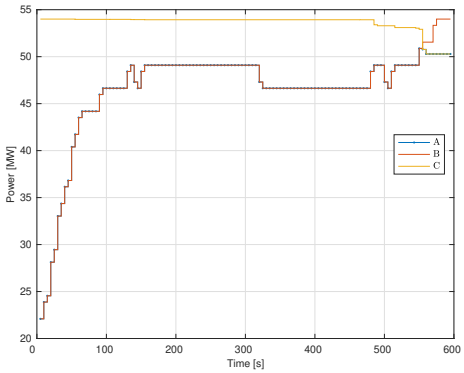

Fig. 4. The power variables in the power generator at node 2745 from the MPC result with prediction horizon N=3. A) $P_n^G(k)$; B) $P_n^A(k)$; C) $\overline{P}_n^G - P_n^C(k)$.

Simulation time is 600 s, and the sampling time is 5 s. For control purposes, the value of $\Delta P_n^G(k)$ is considered constant for each sampling k in the prediction horizon (as pointed out by Figure 8). Moreover, the choice $\Delta \hat{P}_n^A(k) = \Delta P_n^A(k-1)$ is made for the estimation in (12), in order to comply with the "information available". A comparison between the open loop and closed loop system is provided, according to the available power in Figure 2. The open loop system violates the power constraints on two branches (see Figure 3), then requiring to operate on the storage devices and/or on the power curtailment. The power flow on the branch between buses 2745 and 1445 as well as the one between buses 2135 and 2076 trespass the maximum and minimum values. It happens in the time interval after 500 s and up to the end of the simulation for both, while also around 150 s for the branch between buses 2745 and 1445.

The closed loop simulation considers a prediction horizon of 3 steps (i.e. 15 s) and operates on both control levers, as depicted by Figures 4 and 5. The yellow line in Figure 4 describes $\overline{P}_n^G - P_n^C(k)$, while the red one represents $P_n^A(k)$, and the dotted blue one is $P_n^G(k)$.

Figure 5 describes the battery power output and its variations. To maintain the maximal branch values below the limitation, the battery power increases from the initial 0 value, to reach the maximum value at 550 s. For the same goal, renewable power curtailment takes place. Figure 6 shows that

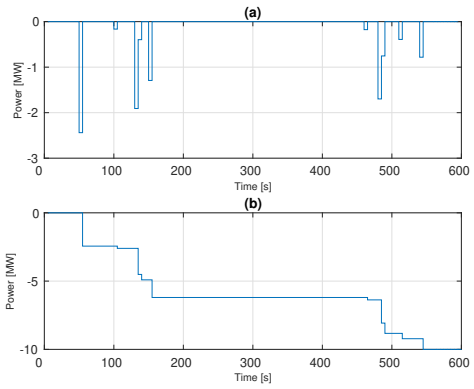

Fig. 5. (a): ΔP_n^B. (b): P_n^B. The prediction horizon is N=3.

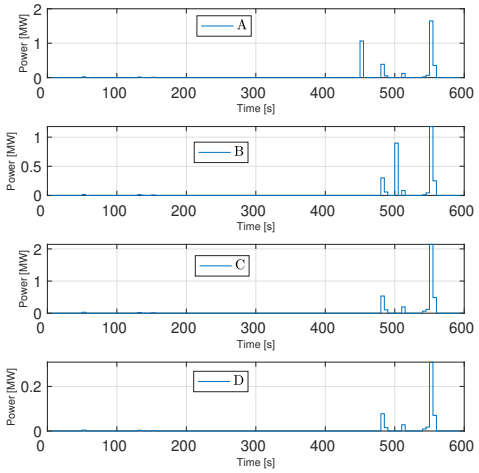

Fig. 6. ΔP_n^C at the generators. The prediction horizon is N=3. A) node 10000; B) node 2076; C) node 2745; D) node 4720.

curtailment correctly occurs later than the battery utilisation, as targeted by the MPC strategy by assigning higher priority to the storage control lever. Indeed, curtailment starts at $t = 450$ s, and increases its value according to the battery power output being saturated. Once the maximum allowed power is reduced such to ensure no power threshold violation on the branches, no curtailment is needed anymore, i.e. after $t = 550$ s. Then, according to the first critical situation depicted in Figure 3 for the branch between buses 2745 and 1445 around $t = 150$ s, it is possible to state that the control action successfully considered only the control degree of freedom given by the battery.

Figure 8 depicts the predictions and computed control actions by MPC on the power flow on the two considered branches. We remark that no hard constraints violation takes place with respect to the predictions $(+/-45MW)$, and no feasibility issues for the real-time solvers appear. On the other hand, these predictions are subject to the uncertainty in the estimation (noticeable for example in Figure (7)) of the power generation. Consequently, they can activate the constraints with anticipation with respect to the real scenario. The choice of the length of the prediction scenario is important in this respect, as it can trigger the control levers in advance. Moreover, a consequence of the model mismatch is the slight difference of the real flow with respect to the

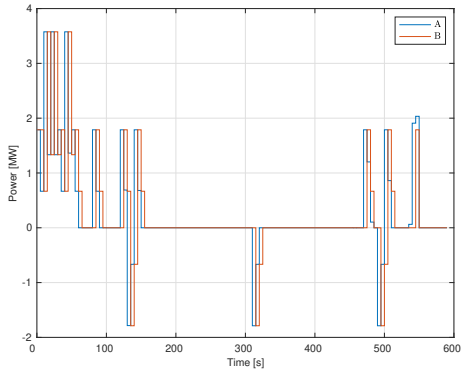

Fig. 7. A) real ΔP_n^G at the node 2745; B) estimated ΔP_n^G at the node 2745.

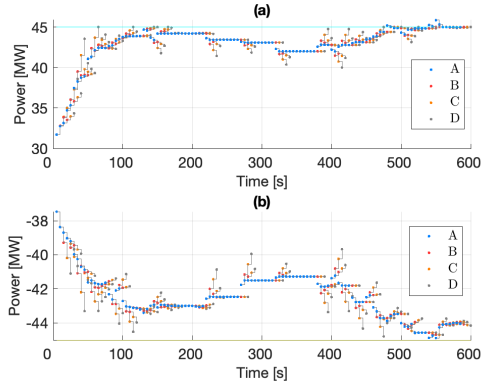

Fig. 8. The power flow on the branches in the closed-loop simulation: (a) between buses 2745 and 1445; (b) between buses 2135 and 2076. A) Power Flow in *runpf*. B) MPC predicting the first step ahead. C) MPC predicting the second step ahead. D) MPC predicting the third step ahead.

predicted one based on PTDF coefficients and subject to uncertainty. This leads to a blue curve which trespass the limitations at several time instants with negligible values. It is interesting to observe the automatic activation of the control action in such situations.

Control with longer prediction horizon: in order to analyse the impact on the proposed approach, we consider a MPC strategy with a longer prediction horizon equal to $N = 10$. The resulting renewable power curtailment is shown in Figure 9. While the constraints satisfaction is validated on the same arguments as in the previous case $N = 3$, the distribution of the power curtailment increments is different and shows a more cautious decision making as a result of the uncertainty propagation. Such prediction windows need to be considered whenever delays in the control actions need to be handled. These studies are subject to current works and will be considered for publication in the near future.

V. Conclusions

A model-based control approach for optimal management of the power flow in a sub-area of a transmission network by the utilisation of storage devices and partial curtailment of the renewable power was presented in this paper. The approach converts the congestion management in a feasibility problem for a feedback control, and has been formulated in terms of a receding horizon optimization. The main contributions are the linear prediction model (with obvious computational advantages) for the evolution of the power as well as the uncertainty handling for the satisfaction of the constraints on power lines. Simulation results confirm the MPC to be an adequate control technique for zonal transmission networks.

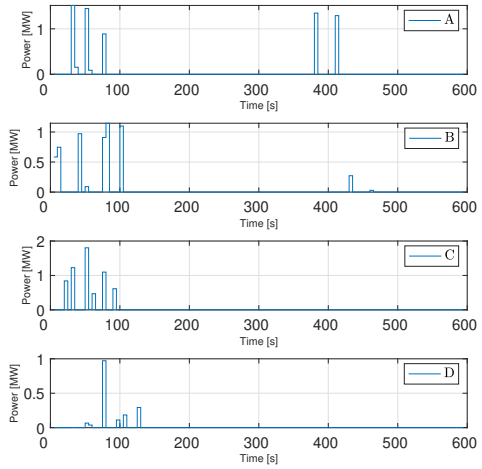

Fig. 9. Control actions for curtailment when prediction horizon N=10. A) node 10000; B) node 2076; C) node 2745; D) node 4720.

References

[1] B. Meyer, J. Astic, P. Meyer, F. Sardou, C. Poumarede, N. Couturier, M. Fontaine, C. Lemaitre, J. Maeght, and C. Straub, "Power Transmission Technologies and Solutions: The Latest Advances at RTE, the French Transmission System Operator," *IEEE Power and Energy Magazine*, vol. 18, no. 2, pp. 43–52, 2020.

[2] A. Iovine, T. Hoang, S. Olaru, J. Maeght, and P. Panciatici, "Modeling the partial renewable power curtailment for transmission network management," in *IEEE PowerTech Conference*, 2021.

[3] A. J. Wood, B. F. Wollenberg, and G. B. Sheblé, *Power Generation, Operation, and Control, 3rd Edition*. Wiley, 2013.

[4] Xu Cheng and T. J. Overbye, "PTDF-based power system equivalents," *IEEE Transactions on Power Systems*, vol. 20, no. 4, pp. 1868–1876, 2005.

[5] C. Straub, S. Olaru, J. Maeght, and P. Panciatici, "Robust MPC for temperature management on electrical transmission lines," vol. 51, pp. 355 – 360, 2018. 17th IFAC Workshop on Control Applications of Optimization CAO 2018.

[6] C. Straub, S. Olaru, J. Maeght, and P. Panciatici, "Zonal congestion management mixing large battery storage systems and generation curtailment," in *2018 IEEE Conference on Control Technology and Applications (CCTA)*, pp. 988–995, 2018.

[7] E. F. Camacho and C. Bordons, *Model predictive control*. Springer, 2007.

[8] B. Otomega, A. Marinakis, M. Glavic, and T. Van Cutsem, "Emergency alleviation of thermal overloads using model predictive control," in *2007 IEEE Lausanne Power Tech*, pp. 201–206, 2007.

[9] R. Gupta, F. Sossan, and M. Paolone, "Performance assessment of linearized opf-based distributed real-time predictive control," in *2019 IEEE Milan PowerTech*, pp. 1–6, 2019.

[10] R. D. Zimmerman, C. E. Murillo-Sánchez, and R. J. Thomas, "Matpower: Steady-state operations, planning, and analysis tools for power systems research and education," *IEEE Transactions on Power Systems*, vol. 26, no. 1, pp. 12–19, 2011.

[11] C. Josz, S. Fliscounakis, J. Maeght, and P. Panciatici, "AC Power Flow Data in MATPOWER and QCQP Format: iTesla, RTE Snapshots, and PEGASE," 2016. https://arxiv.org/abs/1603.01533.

[12] C. Straub, J. Maeght, C. Pache, P. Panciatici, and R. Rajagopal, "Congestion management within a multi-service scheduling coordination scheme for large battery storage systems," in *2019 IEEE Milan PowerTech*, pp. 1–6, 2019.

[13] J. Löfberg, "Yalmip : A toolbox for modeling and optimization in matlab," in *In Proceedings of the CACSD Conference*, (Taipei, Taiwan), 2004.